Blocking IL-1β reverses the immunosuppression in mouse breast cancer and synergizes with anti–PD-1 for tumor abrogation

Irena Kaplanov[a], Yaron Carmi[a,1], Rachel Kornetsky[a], Avishai Shemesh[a,2], Galina V. Shurin[b,c], Michael R. Shurin[b,c], Charles A. Dinarello[d,e,3], Elena Voronov[a], and Ron N. Apte[a,3]

[a]The Shraga Segal Department of Microbiology, Immunology and Genetics, Faculty of Health Sciences, Ben-Gurion University of the Negev, Beer-Sheva 84105, Israel; [b]Department of Pathology, University of Pittsburgh Medical Center, Pittsburgh, PA 15261; [c]Department of Immunology, University of Pittsburgh Medical Center, Pittsburgh, PA 15213; [d]Department of Medicine, University of Colorado, Aurora, CO 80045; and [e]Department of Medicine, Radboud University Medical Center, 6525 GA Nijmegen, The Netherlands

Contributed by Charles A. Dinarello, November 10, 2018 (sent for review July 19, 2018; reviewed by Sebastian Kobold and Karolina Palucka)

Interleukin-1β (IL-1β) is abundant in the tumor microenvironment, where this cytokine can promote tumor growth, but also antitumor activities. We studied IL-1β during early tumor progression using a model of orthotopically introduced 4T1 breast cancer cells. Whereas there is tumor progression and spontaneous metastasis in wild-type (WT) mice, in IL-1β–deficient mice, tumors begin to grow but subsequently regress. This change is due to recruitment and differentiation of inflammatory monocytes in the tumor microenvironment. In WT mice, macrophages heavily infiltrate tumors, but in IL-1β–deficient mice, low levels of the chemokine CCL2 hamper recruitment of monocytes and, together with low levels of colony-stimulating factor-1 (CSF-1), inhibit their differentiation into macrophages. The low levels of macrophages in IL-1β–deficient mice result in a relatively high percentage of $CD11b^+$ dendritic cells (DCs) in the tumors. In WT mice, IL-10 secretion from macrophages is dominant and induces immunosuppression and tumor progression; in contrast, in IL-1β–deficient mice, IL-12 secretion by $CD11b^+$ DCs prevails and supports antitumor immunity. The antitumor immunity in IL-1β–deficient mice includes activated $CD8^+$ lymphocytes expressing IFN-γ, TNF-α, and granzyme B; these cells infiltrate tumors and induce regression. WT mice with 4T1 tumors were treated with either anti–IL-1β or anti–PD-1 Abs, each of which resulted in partial growth inhibition. However, treating mice first with anti–IL-1β Abs followed by anti–PD-1 Abs completely abrogated tumor progression. These data define microenvironmental IL-1β as a master cytokine in tumor progression. In addition to reducing tumor progression, blocking IL-1β facilitates checkpoint inhibition.

immunotherapy | IL-1β | breast cancer | anti–PD-1 | antitumor immunity

The tumor microenvironment is complex and consists of various subsets of stromal, innate, and adaptive immune cells, each of which communicates with the malignant cells and among themselves through a network of growth factors, cytokines, chemokines, adhesion molecules, and extracellular matrix components (1–4). Inflammation of the "wound-healing" type, which promotes invasiveness and concomitantly induces immunosuppression, is one of the hallmarks of the microenvironment of progressing tumors.

In experimental tumor models, but also in patients who have cancer, there is often a correlation between the abundance of specific subsets of tumor-infiltrating leukocytes or stromal cells in the tumor microenvironment and disease outcome (5–7). For example, macrophages mainly of the M2 phenotype, immature myeloid cells [also termed myeloid-derived suppressor cells (MDSCs)], neutrophil subsets, regulatory dendritic cells (DCs), and regulatory T cells are associated with tumor progression (8–19). In contrast, infiltration of tumors with effector Th1 cells, cytotoxic T cells, B cells, and DCs is associated with better clinical outcomes, likely due to development of antitumor immunity (5–7). In advanced tumors, immunostimulatory cells coexist in the tumor microenvironment with immunosuppressive cells. However, due to the dominant function of immunosuppression, tumors progress. For effective adaptive antitumor immunity, immunosuppression needs to be ablated or largely reduced.

IL-1α and IL-1β are "upstream" proinflammatory cytokines, which also activate adaptive immune responses under certain conditions (reviewed in refs. 1, 2, 20, 21). Of particular importance to tumor-mediated inflammation is IL-1β, which is the major secreted IL-1 agonist that is abundant in the tumor microenvironment, whereas IL-1α is mainly cell-associated. In the tumor microenvironment, IL-1β is produced by infiltrating myeloid cells, whereas IL-1α is present in epithelial tumor cells. We have previously demonstrated that IL-1β promotes tumorigenesis, tumor invasiveness, and immunosuppression, mainly mediated by inducing MDSCs (22–24; reviewed in refs. 2, 20). Indeed, IL-1β is increased in most cancers, including breast cancer in

Significance

Inflammation and immunosuppression are dominant features of cancer progression. In the tumor microenvironment, macrophages produce interleukin-1β (IL-1β), which subsequently recruits myeloid cells from the bone marrow. In mice deficient in IL-1β or in wild-type mice treated with anti–IL-1β Abs, implanted breast cancer tumors regress. Regression is due to decreased tumor-related immunosuppression, meditated mainly by macrophages, and increased antitumor immunity, mediated by elevated dendritic cell function and activated cytotoxic CD8 lymphocytes. Although anti–PD-1 reduces tumor growth, the combination of anti–IL-1β plus anti–PD-1 abrogated the tumors completely. These observations support clinical trials of blocking IL-1β in cancer and that anti–IL-1β is a checkpoint inhibitor.

Author contributions: I.K., Y.C., G.V.S., M.R.S., C.A.D., E.V., and R.N.A. designed research; I.K., Y.C., and R.K. performed research; I.K. and A.S. contributed new reagents/analytic tools; I.K., Y.C., R.K., C.A.D., E.V., and R.N.A. analyzed data; and I.K., C.A.D., E.V., and R.N.A. wrote the paper.

Reviewers: S.K., Klinikum der Ludwig-Maximilians-Universität München; and K.P., The Jackson Laboratory for Genomic Medicine.

The authors declare no conflict of interest.

See Commentary on page 1087.

[1]Present address: Department of Human Pathology, The Sackler School of Medicine, Tel Aviv University, Ramat Aviv, Israel 6997801.

[2]Present address: Department of Microbiology and Immunology, The Parker Institute for Cancer Immunotherapy, University of California, San Francisco, CA 94143.

[3]To whom correspondence may be addressed. Email: rapte@bgu.ac.il or cdinare333@aol.com.

This article contains supporting information online at www.pnas.org/lookup/suppl/doi:10.1073/pnas.1812266115/-/DCSupplemental.

Published online December 13, 2018.

advanced stages, where it is mainly expressed by cells in the microenvironment and enhances progression and metastasis (25–31). Moreover, IL-1β limits the antitumor efficacy of certain chemotherapeutic agents (32) and is essential for IL-22, a cancer-promoting cytokine, production (33). However, IL-1β can also promote adaptive T cell-mediated immunity (34) and serves as an adjuvant for expansion and maturation of $CD4^+$ and $CD8^+$ T cells. Changing the tumor microenvironment from one of proinvasive inflammation into one of functional antitumor cell immunity before overt immunosuppression prevails is a major objective of treating cancer (35–37). Support for this concept comes from a recent trial blocking IL-1β in a randomized, placebo-controlled trial in over 10,000 patients at high risk for lung cancer (38).

We were among the first to show that reduction of IL-1β in mouse tumors alleviated tumor progression (22–24; reviewed in ref. 1). Using the 4T1 experimental mouse model of triple-negative breast cancer (TNBC), we investigated the role of microenvironment-derived IL-1β on tumor–host interactions. Treatment of 4T1 tumors with anti–IL-1β Abs facilitates the development of adaptive antitumor cell immunity, and the antitumor cell efficacy of anti–IL-1β Abs significantly potentiated checkpoint inhibition by anti–PD-1.

Results

IL-1β Regulates the Growth of the Murine 4T1 Mammary Carcinoma. Using orthotropic injection of 4T1 breast cancer cells in wild-type (WT) BALB/c mice, progressive tumor growth and 100% mortality were observed around 45 d after tumor cell inoculation (Fig. 1 *A* and *B*). Spontaneous lung metastases developed after day 25 in all WT mice (Fig. 1*C*). In contrast, injection of 4T1 cells into IL-1β–deficient mice resulted in initial tumor growth followed by regression, which started around day 12. By day 20–25, no visible tumors were observed. All IL-1β KO mice in which tumors regressed remained tumor-free and without lung metastases for at least 10 mo, when the experiment was terminated.

To further assess an essential role for IL-1β in tumor progression, we injected 4T1 cells into BALB/c mice, which were simultaneously treated with either anti–IL-1β or control isotypic Abs. Neutralization of IL-1β in BALB/c mice injected with 4T1 cells dramatically reduced the rate of tumor growth, while irrelevant Abs had no effect (Fig. 1*D*). We next injected 4T1 tumor cells that overexpress and secrete IL-1β (4T1–IL-1β) into IL-1β–deficient mice and observed progressive tumor growth. Moreover, tumor development in IL-1β–deficient mice was comparable to tumor development in BALB/c mice (Fig. 1*E*).

We also used the TNBC polyoma middle-T antigen (PyMT) cell line derived from C57BL/6 mice, which was derived from mice transgenic for expression of PyMT in the mammary glands. As shown in Fig. 1*F*, tumor progression of the PyMT cell line in IL-1β–deficient mice of C57BL/6 origin was significantly reduced compared with tumors in WT C57BL/6 mice. These data also support the concept that IL-1β in the tumor milieu significantly contributes to tumor progression and that neutralization or reduction of IL-1β reduces invasiveness or leads to tumor regression.

Microenvironment IL-1β Determines the Nature of Myeloid Cells in Tumor Sites. To elucidate the mechanisms through which IL-1β promotes tumor progression, we analyzed the nature of innate immune cells in the tumor microenvironment of 4T1 tumors obtained from BALB/c and IL-1β–deficient mice. As indicated, regression of 4T1 tumors in IL-1β–deficient mice begins after day 12 (Fig. 1*A*). Before that time, the kinetics of 4T1 tumor development and the size of tumors are similar in both strains of mouse. Thus, we analyzed changes in immune cells comparing 4T1 tumors in BALB/c and IL-1β–deficient mice on day 12.

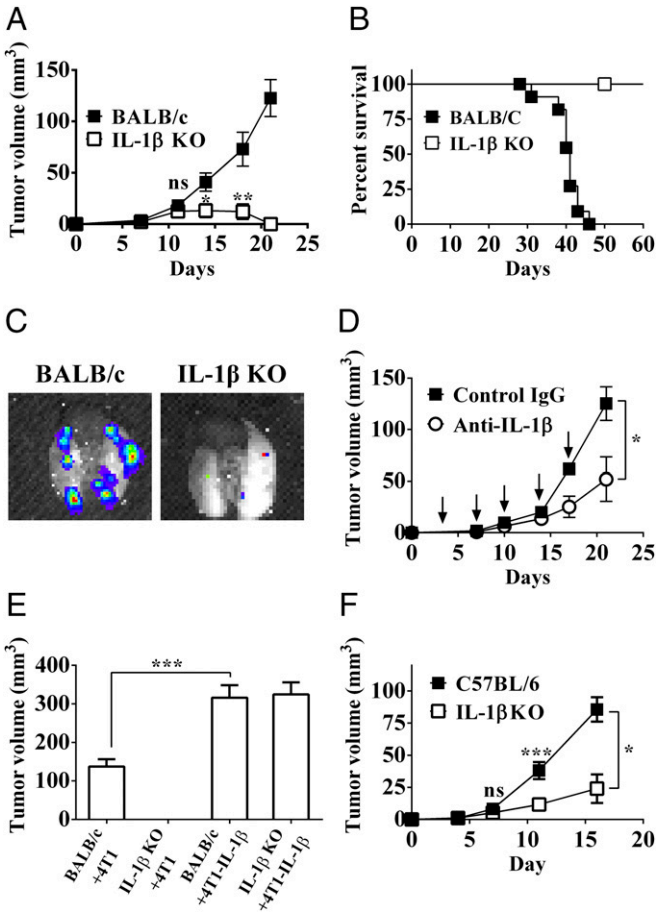

Fig. 1. IL-1β regulates mammary tumor growth and invasiveness. Tumor growth in BALB/c and IL-1β–deficient mice (IL-1β KO). A total of 2×10^5 4T1 cells were injected orthotopically into the mammary fat pad of either BALB/c (■) or IL-1β KO (□) mice as described (*Materials and Methods*). Tumor volume (*A*) and mouse survival (*B*) were monitored every 3–4 d ($n = 6$–12). (*C*) Lungs from BALB/c and IL-1β KO mice imaged ex vivo by an IVIS system 35 d after injection with 4T1-Luc cells. (*D*) Influence of IL-1β neutralization on 4T1 tumor growth. Tumor-bearing BALB/c mice were treated with either isotypic Abs (■) or anti–IL-1β Abs (○) twice a week from day 0 (downward arrows), and tumor volume was measured every 3–4 d as described (*Materials and Methods*; $n = 3$–10). (*E*) Primary tumor volume in BALB/c and IL-1β KO mice on day 21 after injection of 4T1 cells or IL-1β–overexpressing cells (4T1–IL-1β). (*F*) PyMT cells (2×10^5) were injected orthotopically into the mammary fat pads of either C57BL/6 (■) or C57BL/6-IL-1β KO (□) mice. Tumor volumes were monitored every 3–4 d. Graphs show mean ± SEM ($n = 3$–8). *$P < 0.05$; **$P < 0.01$; ***$P < 0.001$. ns, not significant.

Dissected tumors were digested into single cells and subjected to flow cytometry to characterize myeloid cells. The gating scheme to define myeloid cells from tumor cell suspensions and the markers for their characterization are shown in *SI Appendix*, Figs. S1 and S2. Most (80%) of the infiltrating leukocytes ($CD45^+$ cells) were of myeloid cell origin (*SI Appendix*, Fig. S3 *A* and *B*). We did not observe differences in the inflammatory monocytes ($SSC^{low}CD11b^+Ly6C^{high}Ly6G^-MHCII^-$) between BALB/c and IL-1β–deficient mice (*SI Appendix*, Fig. S3 *C* and *D*).

However, we did observe significant differences in cell populations originating from inflammatory monocytes, for example, macrophages with markers $SSC^{low}CD11b^+Ly6G^-CD64^+MHCII^{-/+}$ or $CD11b^+$ DCs with markers $SSC^{low}CD11b^+Ly6C^-CD64^-MHCII^+$. The absolute number of macrophages was

significantly higher in BALB/c mice (35,013 ± 2,726 cells) compared with IL-1β–deficient mice (11,842 ± 2,477 cells) (Fig. 2*A*, *Left*), whereas the number of CD11b$^+$ DCs was the same in tumors in both strains of mice (Fig. 2*A*, *Right*). Also, the percentage of macrophages among CD11b$^+$ tumor-infiltrating cells was significantly higher in BALB/c mice compared with IL-1β–deficient mice (23.92 ± 2.752% and 6.992 ± 1.181%, respectively; Fig. 2*B*, *Left*).

We next injected IL-1β–secreting tumor cells (IL-1β–4T1) into IL-1β–deficient mice. As shown in Fig. 2*B*, *Left*, the percentage of macrophages was similar to that observed in BALB/c mice injected with 4T1 cells and also to that observed in BALB/c mice injected with IL-1β–4T1 cells. In fact, the percentage CD11b$^+$ DCs among CD11b$^+$ tumor-infiltrating cells was significantly higher in IL-1β–deficient mice in comparison to BALB/c mice (25.75 ± 3.28% and 11.05 ± 2.298%, respectively; Fig. 2*B*, *Right*). Furthermore, in IL-1β–deficient mice, as well as in BALB/c mice that received IL-1β–4T1 cells, we observed CD11b$^+$ DCs levels even lower than those in BALB/c mice injected with 4T1 cells. The same phenomenon, of reduced macrophage levels in IL-1β KO mice, was observed in PyMT tumors, while there was no difference in CD11b$^+$ DCs between the C57BL/6 and IL-1β KO mice (Fig. 2*C*). Furthermore, when BALB/c mice bearing 4T1 tumors were treated with anti–IL-1β Abs, a significant decrease in the percentage of macrophages and an increase in the percentage of CD11b$^+$ DCs were observed in tumor infiltrates, similar to those found in IL-1β–deficient mice (Fig. 2*D*). These findings are consistent with the concept that in the tumor microenvironment, IL-1β plays an important role in determining of nature of myeloid cell infiltrates.

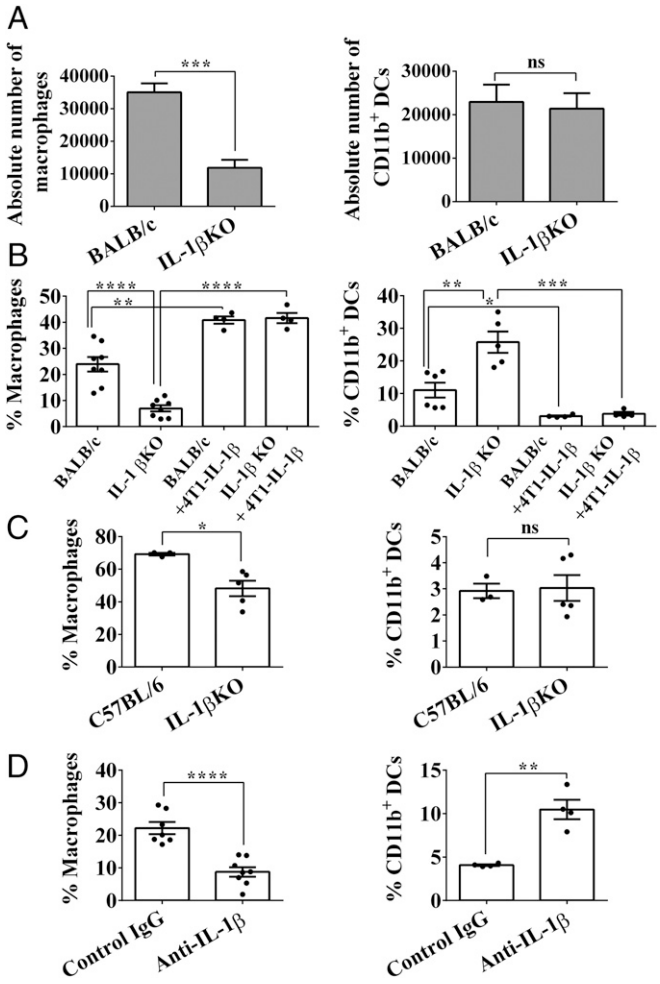

Fig. 2. IL-1β affects the nature of myeloid cells in the mammary tumors. On day 12 after 4T1 cell injection, BALB/c and IL-1β KO mice were killed and single-cell suspensions from primary tumors were prepared as described (*Materials and Methods*). (*A*) Absolute number of macrophages (*Left*) and CD11b$^+$ DCs (*Right*) was calculated from 100,000 CD11b$^+$Ly6G$^-$SSC^{low} cells in tumors. (*B*) Percentage of macrophages (*Left*; CD11b$^+$Ly6G$^-$SSC^{low}CD64$^+$Ly6C$^-$MHCII$^{+/-}$) and CD11b$^+$ DCs (*Right*; CD11b$^+$Ly6G$^-$SSC^{low}CD64$^+$Ly6C$^-$MHCII$^{+/-}$) in extracted tumors. Graphs show the percentage from CD11b$^+$Ly6G$^-$SSC^{low} cells. (*C*) Percentage of macrophages (*Left*) and CD11b$^+$ DCs (*Right*) in extracted 16-d old PyMT tumors. Graphs show the percentage from CD11b$^+$Ly6G$^-$SSC^{low} cells. (*D*) BALB/c mouse treatment with either isotypic or anti–IL-1β Abs. On day 12, tumor single-cell suspensions were stained for macrophages (*Left*) or CD11b$^+$ DCs (*Right*). Graphs show percentage from CD11b$^+$Ly6G$^-$SSC^{low} cells. All graphs show mean ± SEM (n = 3–8). *P < 0.05; **P < 0.01; ***P < 0.001; ****P < 0.0001. ns, not significant.

IL-1β Promotes Recruitment of Cells Positive for C-C Chemokine Receptor Type 2 to the Mammary Tumor Site Through CCL2. Inflammatory monocytes, as well as macrophages and CD11b$^+$ DCs, express the C-C chemokine receptor type 2 (CCR2) (*SI Appendix*, Fig. S2). We found that among tumor-derived CD11b$^+$ cells, the fraction of CCR2$^+$ cells is dramatically decreased in IL-1β–deficient mice compared with BALB/c mice: 9.45 ± 1.95% versus 34.78 ± 4.64%, respectively (Fig. 3*A*). CCR2 is the receptor of several chemokines, including CCL2 (MCP-1), CCL7 (MCP-3), and CCL13 (reviewed in ref. 39). Previously, CCL2 has been implicated as the major ligand that attracts cells of the macrophage lineage to inflamed tissues (reviewed in ref. 40). Indeed, a significantly lower level of CCL2 was measured in tumor tissues from IL-1β–deficient mice (20.04 ± 8.841 pg/mg of protein) compared with the levels in tumors obtained from BALB/c mice (210.7 ± 34.41 pg/mg of protein) (Fig. 3*B*). In addition, treatment of tumor-bearing BALB/c mice with anti–IL-1β Abs markedly reduced CCL2 levels in tumor extracts (72.25 ± 23.59 pg/mg of protein) (Fig. 3*B*).

We next corroborated these findings with data from The Cancer Genome Atlas (TCGA) in a cohort of 1,215 patients with breast cancer. There is a significant direct correlation between IL-1β and CCL2 expression levels (R^2 = 0.4351), but not with other CCR2 ligands, such as CCL7 (R^2 = 0.06778) and CCL13 (R^2 = 0.1040) (Fig. 3*C*). Taken together, these data confirm that in the 4T1 tumor model, as well as in patients with breast cancer, recruitment of inflammatory monocytes into tumor sites is regulated by IL-1β, most probably through CCL2 induction.

IL-1β Controls the Differentiation of Macrophages in Breast Tumor Sites. To study the effects of microenvironmental IL-1β on the differentiation of inflammatory monocytes in vivo, we devised an experimental setting to study the direct effects of tumor-derived mediators on the maturation of monocytes. Seven days after the injection of tumor cells, at a time when primary tumors were visible, freshly isolated naive blood monocytes from BALB/c or IL-1β KO mice were mixed with Matrigel and injected into mice near the margins of 4T1 tumors in BALB/c or IL-1β KO mice, respectively. At different intervals thereafter, Matrigel plugs were recovered from tumor-bearing mice, and monocytes, macrophages, and CD11b$^+$ DCs were characterized by flow cytometry. In Matrigel plugs implanted into tumor-free naive mice, almost no macrophage differentiation was observed (3.56% after 72 h; Fig. 4*A*, *Left*). However, we observed that in Matrigel plugs obtained from tumor-bearing BALB/c mice, there is a time-dependent increase in the number of mature macrophages. For example, after 72 h, 53.1% of the cells in the plugs are macrophages, whereas only a limited number of mature macrophages were observed in tumors in IL-1β–deficient mice (12.1%; P = 0.0321). In Fig. 4*B*, the kinetics of accumulation of macrophages

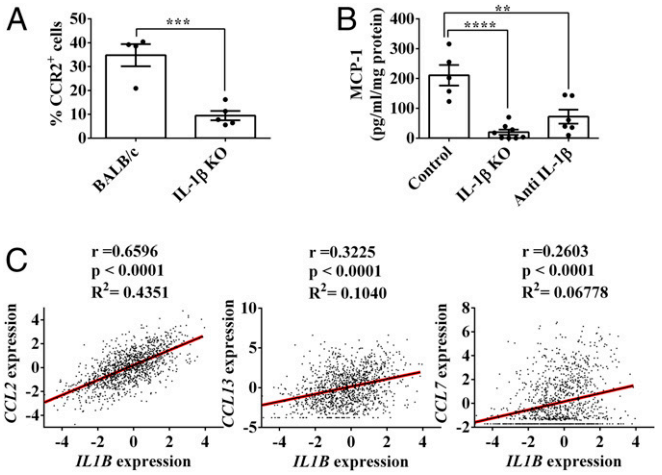

Fig. 3. IL-1β promotes accumulation of tumor-infiltrating CCR2$^+$ cells through MCP-1. On day 12 after 4T1 cell injection, BALB/c and IL-1β KO mice were killed and single-cell suspensions from the primary tumors were prepared as described (*Materials and Methods*). (*A*) Percentage of CCR2$^+$ cells from CD11b$^+$ cells. (*B*) CCL2 protein concentration in 12-d 4T1 tumor extracts, measured by ELISA. Graphs in *A* and *B* show mean ± SEM (n = 4–8). $^{**}P < 0.01$; $^{***}P < 0.001$; $^{****}P < 0.0001$. (*C*) Correlation between *IL1B* expression and different CCR2 ligands (*CCL2*, *CCL13*, and *CCL7*) in human breast cancer samples from the TCGA dataset (n = 1,215).

(Fig. 4*B*, *Left*) and CD11b$^+$ DCs (Fig. 4*B*, *Right*) in Matrigel plugs in BALB/c and IL-1β deficient mice are shown.

The fraction of macrophages increased with time in BALB/c mice and remained low in IL-1β–deficient mice, while the kinetics of CD11b$^+$ DCs were similar in Matrigel plugs adjacent to tumors in both strains of mice. These results demonstrate the effects of microenvironment IL-1β on macrophage differentiation.

Colony-stimulating factor-1 (CSF-1) is the major macrophage maturation factor (41). To test its involvement in macrophage differentiation in 4T1 tumors, we tested its expression levels in day 12 tumors obtained from BALB/c and IL-1β–deficient mice. As shown in Fig. 4*C*, indeed, expression levels of CSF-1 were significantly lower in IL-1β–deficient mice compared with those in tumors in BALB/c mice. Using TCGA-derived data, a positive correlation was found between levels of expression of IL-1β and CSF-1 ($R^2 = 0.3150$, $P < 0.0001$) in tumor samples obtained from patients with cancer (Fig. 4*D*). In contrast, no correlation was found for Fms-related tyrosine kinase 3 ligand (FLT3LG; $R^2 = 0.03714$, $P < 0.0001$) and CSF-2 ($R^2 = 0.1419$, $P < 0.0001$), two growth factors that are involved in DC maturation (reviewed in ref. 42). Thus, in the microenvironment, IL-1β recruits inflammatory monocytes, through induction of CCL2, but it also promotes their maturation into macrophage, probably through CSF-1 induction.

Regression of 4T1 Tumors in IL-1β KO Mice Is Dependent on CD8$^+$ T Cells. We examined the influence of microenvironmental IL-1β on induction and activity of antitumor CD8$^+$ T cell-mediated adaptive immunity. We analyzed tumors obtained on day 12 by fluorescence-activated cell sorting (FACS), which revealed that the frequency of CD8$^+$ T cells among CD3$^+$ T cells is sevenfold higher in tumors obtained from IL-1β–deficient mice compared with tumors from BALB/c mice (Fig. 5*A*). This difference was also observed by immunostaining (Fig. 5*B*), where there are large numbers of CD8$^+$ T cells in tumors from IL-1β–deficient mice, while these cells are scarce in tumors from BALB/c mice.

Next, we assessed if CD8$^+$ T cells are responsible for tumor regression observed in IL-1β KO mice. As shown in Fig. 5*C*, when CD8$^+$ T cells were depleted, tumor regression was abrogated in IL-1β–deficient mice ($P = 0.007$ on day 28). On day 28, the mean tumor volume was similar in BALB/c and IL-1β–deficient mice treated with anti-CD8$^+$ Abs ($P = 0.9927$). Depletion of CD8$^+$ T cells also increased primary tumor growth in BALB/c mice compared with control: 71.47 ± 6.991 mm^3 and 37.33 ± 4.068 mm^3, respectively ($P = 0.0124$).

The functional parameters related to tumor-infiltrating CD8$^+$ T cells were assessed using intracellular staining of IFN-γ and TNF-α. We observed higher intracellular expression levels of these cytokines in CD8$^+$ T cells from tumors in IL-1β–deficient mice compared with tumors in BALB/c mice (Fig. 5*D*). Moreover, expression levels of granzyme B, a molecule that mediates CD8$^+$ T cell killing of target cells, were threefold higher in tumors in IL-1β–deficient mice compared with tumors in BALB/c mice (Fig. 5*E*). Thus, increased expression of granzyme B per

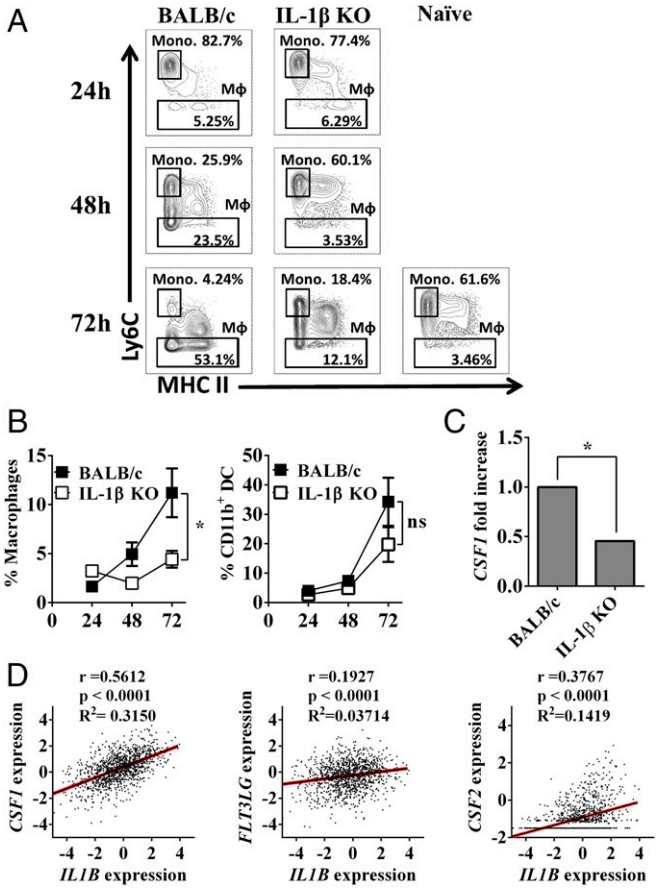

Fig. 4. IL-1β promotes tumor-infiltrating inflammatory monocyte (Mono.) differentiation to macrophages. On day 7 after 4T1 cell injection, BALB/c and IL-1β KO mice were injected with 50 μL of liquid Matrigel mixed with 200,000 blood mononuclear cells extracted from naive BALB/c or IL-1β KO mice, respectively. Mice were killed 24 h, 48 h, and 72 h after Matrigel plug transplantation, and single-cell suspensions from Matrigel plugs were prepared as described (*Materials and Methods*). (*A*) Representative contour plot of CD11b$^+$Ly6G$^-$SSC^{low}Ly6C$^{+/-}$/CD64$^+$ cells in BALB/c and IL-1β KO mice. (*B*) Percentage of mature macrophages (CD11b$^+$Ly6G$^-$SSC^{low}Ly6C$^-$CD64$^+$MHCII$^{+/-}$) in Matrigel plugs from CD11b$^+$ cells (*Right*) and percentage of CD11b$^+$ DCs (CD11b$^+$Ly6G$^-$SSC^{low}Ly6C$^-$CD64$^-$MHCII$^+$) in Matrigel plugs from CD11b$^+$ cells (*Left*). Graphs show mean ± SEM (n = 3–4). $^*P < 0.05$. ns, not significant. (*C*) Expression of the *CSF1* gene in 12-d 4T1 tumors from BALB/c and IL-1β KO mice was assessed using qPCR. Gene expression was normalized based on the expression of *ACTB*. The graph shows mean ± SEM (n = 3). $^*P < 0.05$. (*D*) Correlation between *IL1B* expression and *CSF1*, *FL3LG*, and *CSF2* in human breast cancer samples from the TCGA dataset (n = 1,215).

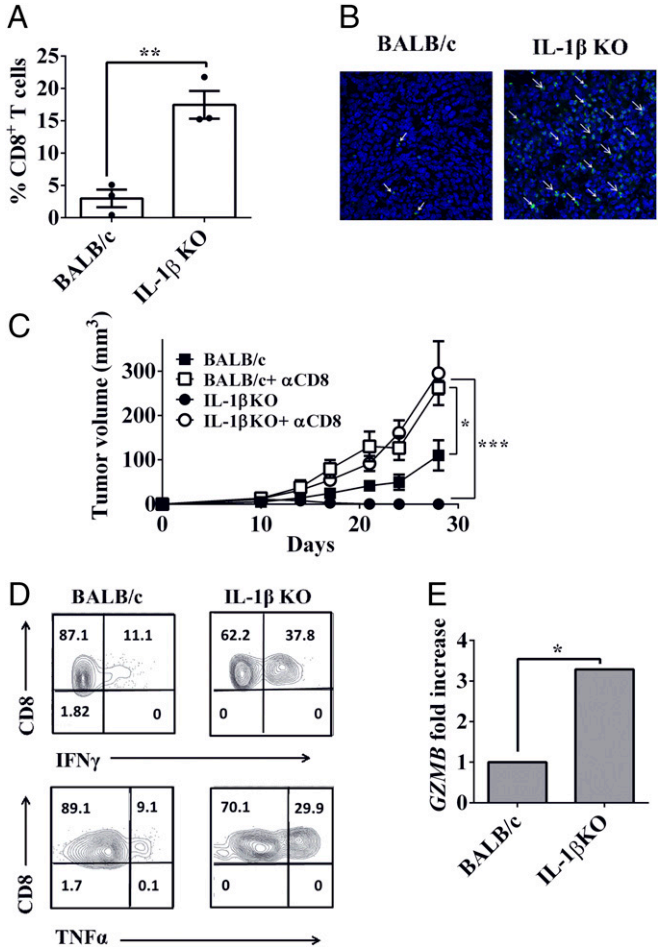

Fig. 5. Tumor regression in IL-1β KO mice is $CD8^+$ T cell-dependent. BALB/c and IL-1β KO mice were injected with 2×10^5 4T1 cells. The 4T1-bearing BALB/c and IL-1β KO mice were killed on day 12 after injection of 4T1 cells. (*A*) Percentage of $CD8^+$ T cells from $CD3^+$ cells in primary tumor single-cell suspensions ($n = 3$). (*B*) Histological section from primary tumor stained with anti-CD8 Abs (green) and DAPI (blue). (Magnification: *B*, 60×.) (*C*) Depletion of $CD8^+$ cells was achieved by multiple i.p. injections of anti-CD8 Abs. Primary tumor volumes of BALB/c mice (■), BALB/c mice treated with anti-CD8 Abs (□), IL-1β KO mice (●), and IL-1β KO mice treated with anti-CD8 Abs (○) are shown. Tumor volume was measured every 3–4 d as described (*Materials and Methods*; $n = 4$–5). (*D*) Representative contour plot of intracellular production of IFN-γ and TNF-α by tumor-derived $CD8^+$ T cells. (*E*) Expression of *GZMB* gene in 12-d 4T1 tumors from BALB/c and IL-1β KO mice was assessed using qPCR. Gene expression was normalized based on the expression of *CD8A* ($n = 3$). Graphs show mean ± SEM. $^*P < 0.05$; $^{**}P < 0.01$; $^{***}P < 0.0007$.

$CD8^+$ T cell is higher in IL-1β–deficient mice compared with $CD8^+$ T cells in BALB/c mice bearing 4T1 tumors.

Changes in the IL-12/10 Balance Occur During the Regression of 4T1 Tumors in IL-1β KO Mice. The balance between IL-12 and IL-10 is crucial for the development of antitumor cell adaptive immunity. Therefore, we analyzed patterns of intracellular expression of these cytokines in tumor-derived myeloid cells obtained from tumor-bearing BALB/c and IL-1β–deficient mice. IL-10 was detected only in macrophages in the subset of $MHCII^{low}$ cells (Fig. 6*A*, *Upper*), whereas IL-12 was detected only in $CD11b^+$ DCs (Fig. 6*A*, *Lower*). IL-10 expression levels were detectable mostly in $MHCII^{low}$ macrophages in BALB/c mice (Fig. 6*B*). In contrast, IL-12 expression was only detected in $CD11b^+$ DCs from IL-1β KO mice (Fig. 6*C*). Thus, in 4T1 tumors in BALB/c mice, the ratio between IL-12/IL-10 is in favor of immunosuppression, with high IL-10 and low IL-12 levels. In contrast, in IL-1β–deficient mice, the opposite ratio was observed, favoring antitumor immunity.

We next treated BALB/c mice bearing 4T1 tumors with anti–IL-10 Abs. As shown in Fig. 6*D*, there is a significant decrease in tumor weight and a concomitant elevation in expression of genes related to T cell number or function (i.e., *CD8A*, *GZMB*) (Fig. 6*E*). The elevated T cell genes, after anti–IL-10 treatment, were in line with the elevation of both *IL12A* and *IL12B* genes (Fig. 6*F*), similar to IL-1β KO mice. Furthermore, in the PyMT model, reduced expression of *IL10* gene and elevated expression of *GZMB* gene were also observed in IL-1β KO mice (Fig. 6*G*).

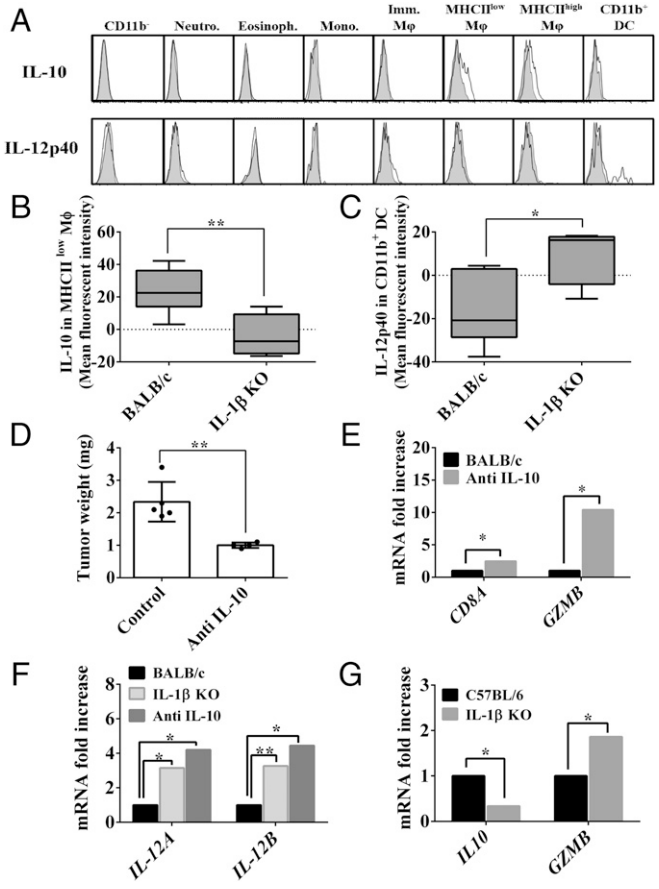

Fig. 6. Macrophage-derived IL-10 leads to tumor promotion through $CD8^+$ T cell suppression. On day 12 after 4T1 cell injection, BALB/c and IL-1β KO mice were killed and single-cell suspensions from the primary tumors were prepared as described (*Materials and Methods*). (*A*) Representative histograms of different cell populations within the primary tumor stained intracellularly with anti–IL-10 Abs, anti–IL-12p40 Abs (white), or isotype control Abs (gray). Imm., immature; Eosinoph., eosinophil; Mono., monocyte; Neutro., neutrophil. Mean fluorescence intensity of anti–IL-10 Abs in MHC^{low} macrophages (*B*) and anti–IL-12p40 Abs in $CD11b^+$ DCs (*C*) ($n = 4$). Tumor-bearing mice were treated i.p. with anti–IL-10 or control IgG Abs (*Materials and Methods*). After 14 d, mice were killed. (*D*) Primary tumor weight ($n = 4$). (*E*) Expression of *CD8A* and *GZMB* genes in primary tumors was assessed using qPCR. Gene expression was normalized based on the expression of *ACTB* ($n = 4$). (*F*) Expression of *IL12A* and *IL12B* genes in primary tumors. Gene expression was normalized based on the expression of *ITGAM* ($n = 4$). (*G*) Expression of *IL10* and *GZMB* genes in PyMT tumors. Gene expression was normalized based on the expression of *ACTB*. Graphs show mean ± SEM. $^*P < 0.05$; $^{**}P < 0.01$.

Anti–IL-1β and Anti–PD-1 Abs Have a Synergistic Antitumor Activity. As shown in Fig. 1, treatment with anti–IL-1β Abs only partially inhibited the growth of 4T1 tumors in BALB/c mice. Moreover, treatment with anti–IL-1β Abs during the early stages of tumor development resulted in lower numbers of myeloid cells in the tumor microenvironment, which decreases immunosuppression (Fig. 2*C*). Based on these findings, we hypothesized that IL-1β neutralization would target myeloid cell-mediated immunosuppression, while anti–PD-1 Abs would restore the function of anergized antitumor T cells. Therefore, 4T1 tumor-bearing BALB/c mice were initially treated with anti–IL-1β Abs on days 4 and 7 after tumor cell injection. Subsequently, on day 10, mice received a single injection of anti–PD-1 Abs. As depicted in Fig. 7 *A* and *B*, there was only partial inhibition in tumor growth in mice treated with single agents, but almost complete inhibition of tumor growth in mice treated with combination therapy. In fact, we observed a highly significant inhibition of tumor growth until day 30, when the experiment was terminated. Analyses of resected tumors on day 30 revealed reduced weight of tumors (Fig. 7*B*) concomitant with a significant increase in the amount of infiltrating $CD8^+$ T cells into the tumor site (Fig. 7*C*). These results clearly indicate the antitumor potential of combination therapy consisting of anti–IL-1β blockade followed by anti–PD-1 neutralization.

Discussion

Summary of Major Findings. This study demonstrates that blocking IL-1β enhances antitumor cell immunity. Furthermore, we show the synergistic action of IL-1β inhibition with anti–PD-1 in restoration of T cell-mediated tumor immunity, which has considerable clinical relevance. The mechanisms by which IL-1β contributes to immunosuppression in the tumor microenvironment of primary orthotropic mammary tumors were shown using the 4T1 cell line in BALB/c mice and the PyMT cell line in C57BL/6 mice, which display regression or significantly reduced growth in IL-1β–deficient mice, respectively. Invasiveness of these tumors was largely reduced in BALB/c control mice treated with neutralizing IL-1β Abs. In the tumor microenvironment in IL-1β–deficient mice, $CCR2^+$ infiltrating cells and their differentiation into immunosuppressive macrophages were decreased, whereas $CD11b^+$ DCs were higher. In IL-1β–deficient mice, reduced immunosuppression enabled the development of efficient T cell-mediated immunity, consisting of activated CD8 cytotoxic T cells and elevated levels of IFN-γ, TNF-α, granzyme B, and IL-12 production but decreased IL-10, each contributing to less immunosuppression and greater tumor cell killing. Together, these mechanisms support the primary finding that reduction of IL-1β acts in synergy with anti–PD-1 for optimal tumor killing.

Relationship with Anti–IL-1β in Humans. The antitumor efficiency of anti–IL-1β, shown by us here in murine models, is supported by the worldwide Canakinumab Anti-inflammatory Thrombosis Outcomes Study (CANTOS) in over 10,000 subjects at high risk for a second cardiovascular accident. The patients were treated with anti–IL-1β Abs (canakinumab) every 3 mo for 4 y. The randomized, placebo-controlled trial met the primary and secondary end points to reduce the frequency of a second myocardial infarction and systemic inflammation (38, 43). However, in the treated group, there was a 67% reduction in the incidence of lung cancer and a 77% reduction in the death rate compared with the placebo group. None of the patients had detectable cancer before the onset of the trial. Since many of the 10,000 subjects were smokers, anti–IL-1β treatment likely reduced the inflammation that progresses to carcinogenesis. It is likely that some of the antitumor mechanisms observed in IL-1β–deficient mice or BALB/c mice treated with anti–IL-1β Abs also apply to subjects receiving canakinumab, as antitumor immunity is a mechanism leading initially to either regression or elimination of small tumors.

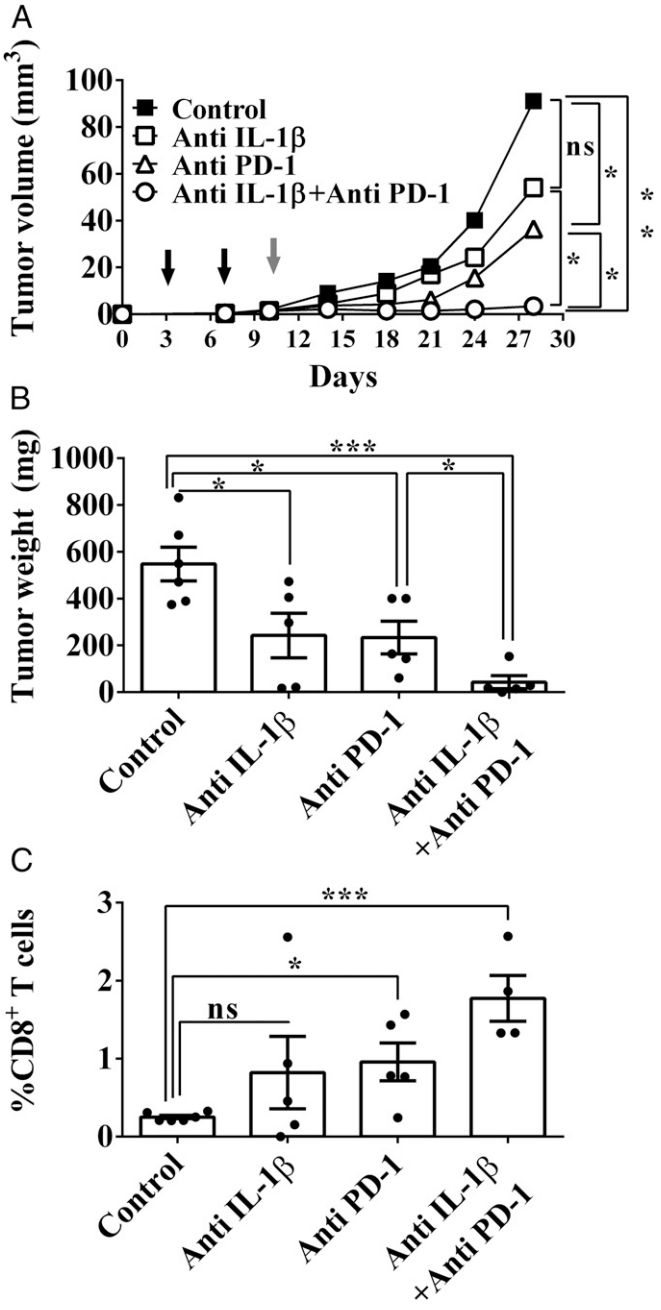

Fig. 7. Combination of anti–IL-1β with anti–PD-1 treatment improves the outcome of 4T1 mammary carcinoma in mice. BALB/c mice were injected with 2×10^5 4T1 cells. On days 4 and 7 after tumor cell injection, some of the mice were injected i.p. with anti–IL-1β or isotype control Abs. On day 10, some mice received a single injection of anti–PD-1 or isotype control Abs. (*A*) Tumor volume of control (■) mice, mice treated with only anti–IL-1β Abs (□), mice treated with only anti–PD-1 Abs (△), and mice treated with both anti–IL-1β and anti–PD-1 Abs (○). On day 30, mice were killed. (*B*) Weight of primary tumors. (*C*) Tumors were enzymatically digested, and cells were analyzed by FACS. The graph shows the percentage of $CD8^+$ T cells from tumor-derived $CD45^+$ leukocytes. All graphs show mean ± SEM (n = 4–6). *$P < 0.05$; ***$P < 0.001$. ns, not significant.

Women with HER2-negative breast cancer have been treated with the naturally occurring IL-1 receptor antagonist (anakinra) for up to 6 mo in combination with a chemotherapeutic agent for breast cancer (29; reviewed in ref. 44). A trial in metastatic colorectal

cancer showed significant survival benefit when anakinra was added to standard-of-care chemotherapy for colorectal cancer (45), and patients with pancreatic cancer also benefit when anakinra is added to chemotherapy (46). The peripheral blood of the patients with HER2-negative breast cancer has an IL-1β transcriptional signature, and levels of IL-1β were elevated in primary breast cancer tissue of 149 patients (29). Of 579 selected immune-related genes in the study, 288 were identified as differentially expressed genes (DEGs) between healthy controls and the patients. Several IL-1–related DEGs were abundant and consistent with an IL-1 transcriptional signature. An IL-1 transcriptional signature was also present in two large breast cancer databases and correlated with poor survival. When treated with anakinra (29; reviewed in ref. 44), there was a significant decrease in the transcriptional signature in the peripheral blood of the patients. Thus, an IL-1–driven inflammatory signature is present in patients with breast cancer with a poor prognosis and can be reduced by blocking IL-1β. The dramatic effects of IL-1 attenuation on progression stem from its broad activities on proinvasive and immunosuppressive inflammation in tumor sites, mainly through induction of genes of cytokines/chemokines and other proinflammatory products in malignant cells or diverse other cells of the microenvironment, such as stromal cells and even epithelial cells.

IL-1β Mediated Immunosuppression Through Its Effects on Myeloid Cell-Infiltrating Tumors. In this study, we observed pronounced differences in $CCR2^+$ myeloid cells and their differentiation progeny [i.e., macrophages (47, 48), $CD11b^+$ DCs (49, 50)] in 4T1 tumors in BALB/c versus IL-1β KO mice. CCL2 represents the major chemokine that recruits inflammatory monocytes, and it also participates in macrophage differentiation (51–53). Another important cytokine affecting macrophage differentiation is CSF-1 (reviewed in ref. 52). Levels of both CCL2 and CSF-1 were reduced in tumors of IL-1β–deficient mice. In another experimental system of breast carcinogenesis and invasiveness, the relationship between IL-1β and CCL2 was also demonstrated (51, 54). However, in that study, CCL2 induced expression of IL-1β in macrophages, which subsequently activated Th17 cells that promote tumor progression (54). In IL-1β–deficient mice, and in tumor-bearing BALB/c mice treated with anti–IL-1β Abs, immunosuppressive myeloid cells and their derived cytokines are reduced, which results in reduced immunosuppression, allowing for effective antitumor cell immunity.

Support of Mouse Data with Human Data from the TCGA Analyses. Many of the findings on IL-1β–induced factors that participate in reprogramming of myeloid cells in the tumor microenvironment in tumor-bearing mice were also corroborated in human breast cancer tumors. A cohort of patients with breast cancer in the TCGA database revealed a linear correlation between levels of IL-1β and CCL2, while there was no significant correlation with other CCR2 ligands (CCL7 and CCL13), which also participate in monocyte recruitment to tumors (reviewed in ref. 55). Furthermore, a direct correlation between expression of IL-1β and CSF-1 was also present, but this correlation was not observed with factors inducing DC maturation (CSF-2 and FLT3LG) (reviewed in ref. 56). The latter observation is in line with the finding that the absolute number of $CD11b^+$ DCs was similar in 4T1 tumors in BALB/c or IL-1β KO mice.

Less IL-1β Results in Greater Antitumor Activity. In IL-1β–deficient mice, the tumor microenvironment contains a heavy and evenly distributed infiltrate of activated $CD8^+$ T cells, as observed by levels of IFN-γ, TNF-α, and granzyme B. Also, $CD8^+$ T cell depletion in IL-1β–deficient mice abolished regression. In contrast, in progressive tumors in BALB/c mice, only scarce $CD8^+$ T cells were observed and activation parameters were lower than in IL-1β–deficient mice. $CD8^+$ T cell activation was facilitated in IL-1β–deficient mice by the significantly reduced macrophage-induced immunosuppression, which is mainly mediated by IL-10 secretion. IL-10 inhibits secretion of IL-12 by DCs (57, 58). In our system, IL-10 is expressed only by macrophages, while IL-12 is expressed only by $CD11b^+$ DCs, as already described (35, 56, 59). IL-10 may act by itself or through PGE2 induction (60), a major immunosuppressive molecule (reviewed in ref. 61). IL-1β was previously shown to be a strong inducer of PGE2 in breast cancer (62). Indeed, anti–IL-10 Abs reduced tumor progression and improved immunological parameters of antitumor T cell responses. The increased proportions of $CD11b^+$ DCs and reduced levels of macrophages in tumors in IL-1β–deficient mice likely contributed to presentation of tumor antigens and antitumor immunity. We think that due to a lower prevalence of macrophages in tumors in IL-1β–deficient mice, the percentage of $CD11b^+$ DCs among myeloid cells is higher. In fact, the 4T1 tumor sites in IL-1β–deficient mice contain high levels of IL-12 and low levels of IL-10, but the opposite cytokine patterns were observed in tumors in BALB/c mice.

Enhancement of Antitumor Activities of Anti–PD-1 by Blocking IL-1β. Neutralization of microenvironment IL-1β in BALB/c-bearing 4T1 tumors reduced tumor growth and improved parameters of antitumor cell immunity but did not result in complete regression. Treatment with anti–IL-1β or anti–PD-1 as a single agent only marginally reduced tumor growth. This prompted us to combine anti–IL-1β treatment with anti–PD-1 treatment. PD-1, expressed on activated T cells (reviewed in refs. 63, 64) mediates anergy of antitumor T cells. Blocking Abs to PD-1 (pembrolizumab and nivolumab) have been broadly used to treat patients with epithelial cancers, leading to reproducible and durable regression of tumors, but only in a fraction of patients with cancer (~20%) (reviewed in refs. 65–67). We observed an impressive synergy with the combination of anti–IL-1β and anti–PD-1 Abs. First, we treated mice with anti–IL-1β Abs 4 and 7 d after tumor cell implantation to reduce the immunosuppression mediated by IL-1β, and thus enable the development of antitumor cell immunity. Subsequently, by blocking PD-1, anergized T cells, which have been previously stimulated, become activated and are recruited to the tumor microenvironment to execute their effector function. This treatment scheme resulted in inhibition of tumor growth for 30 d, at which time the experiment was terminated.

In summary, blocking IL-1β itself results in decreased invasiveness and inflammation-mediated immunosuppression concomitant to increased tumor immunity. When used in combination with a checkpoint inhibitor, IL-1β inhibition enhances restoration of tumor killing without systemic inflammation. The low rate of responses to Abs against immune checkpoint molecules, which is around 20% of durable regressions, is mainly due to the inflammatory and immunosuppressive phenotype of the tumor microenvironment. Alleviating it by IL-1β neutralization can improve this rate of response and prevent the inflammatory side effects of treatments with antiimmune checkpoint Abs. Experiments in our laboratory are aimed at exploring this possibility.

Materials and Methods

Mice. IL-1β–deficient mice (BALB/c and C57BL/6 background) were generated as described (68) and kindly provided by Yoichiro Iwakura, Tokyo University, Tokyo. IL-1β–deficient mice were housed under specific-pathogen-free conditions at the animal facilities of the faculty of Health Sciences, Ben-Gurion University. WT BALB/c and C57BL/6 mice were obtained from Envigo, Israel. Animal studies were approved by the Animal Care Committee of Ben-Gurion University. Female, 8-wk-old mice were used in all experiments.

Cell Lines. The mammary carcinoma cell lines 4T1, 4T1–IL-1β, and 4T1-Luc were received and maintained as described (69). The PyMT cell line was derived from mammary tumors in C57BL/6 mouse mammary tumor virus

(MMTV)-PyMT transgenic mice that express the polyoma middle-T driven by the MMTV promoter (46). It was a kind gift from Ami Aronheim, Technion, Israel Institute of Technology, Haifa, Israel. Cells were cultured in DMEM (GIBCO) using a standard procedure.

Ex Vivo Luminescence. Two hundred microliters of D-Luciferin at a concentration of 15 mg/mL (PerkinElmer) was injected i.p. in parallel with anesthesia. Mice were killed 7 min later, and lungs were promptly removed and imaged with an IVIS system (Caliper LifeSciences, PerkinElmer).

Tumor Models. Cell lines were trypsinized and injected orthotopically (2×10^5 cells per mouse) into a single mammary fat pad of BALB/c (for 4T1, 4T1–IL-1β, and 4T1-Luc) or C57BL/6 (for the PyMT cell line) mice. Neutralizing Abs against IL-1β [10 μg per mouse, i.p. injection (AF-401-NA; R&D Systems)] or IL-10 [0.5 mg per mouse, i.p. injection (JES5-2A5; BioXcell)] were injected twice a week from day 0 after injection of 4T1 cells. Appropriate IgG controls (R&D Systems) were used. Tumor development was measured using a caliper every 3–4 d after injection of tumor cells, and tumor volume was calculated: $(W \times L)^2 \times L$, where W is width and L is length.

Monocyte Differentiation in Matrigel Plugs. BALB/c and IL-β–deficient mice were killed, and blood mononuclear cells were isolated using Ficoll-Paque Plus (Amersham Biosciences). A mixture of 0.5×10^6 blood mononuclear cells and 50 μL of liquid Matrigel (growth factor reduced; R&D Systems) was injected near the margins of the primary 4T1 tumor (BALB/c or IL-β–deficient mice, respectively) on day 7 after tumor cell inoculation. Matrigel plugs were surgically removed after 24 h, 48 h, or 72 h. The plugs were solubilized to assess the composition of containing cells.

Preparation of Single-Cell Suspensions from Primary Tumors and Matrigel Plugs. Primary tumors and Matrigel plugs were obtained from mice and digested using a mixture of enzymes [1 g per 100 mL of collagenase type IV, 20,000 units per 100 mL of DNase type IV, 1 mg/mL of hyaluronidase type V (Sigma–Aldrich) at 37 °C for 20–30 min] as described (70). Single-cell suspensions from tumors were analyzed by FACS or used for RNA isolation. Supernatants from digested tumors were collected and stored at −20 °C for subsequent evaluation.

In Vivo Depletion of $CD8^+$ T Cells. In vivo depletion of $CD8^+$ T cells was performed by i.p. injection of ascitic fluids containing the mAb YTS-169 on days −5, −3, and −1 before inoculation of 4T1 tumor cells and twice per week thereafter. Depletion of the $CD8^+$ T cells in the blood was verified by FACS analysis.

Combined Treatment of Anti–PD-1 and Anti–IL-1β. A total of 2×10^5 4T1 cells were injected, as indicated above, and neutralizing Abs against IL-1β at a rate of 10 μg per mouse (AF-401-NA; R&D Systems) were injected i.p. on days 4 and 7. On day 10, anti–PD-1 Abs at a rate of 200 μg per mouse were injected i.p (RMP1-14; BioXcell). Appropriate control IgG (R&D Systems) Abs were used. Tumor development was measured as described above.

qPCR. Total mRNA was extracted using a RNeasy kit (Qiagen). The quality and amount of extracted RNA were determined using an ND-1000 spectrophotometer (NanoDrop Technologies). cDNA was obtained using a qScript cDNA Synthesis Kit (Quanta Biosciences) according to the manufacturer's instructions. Subsequent qPCR was performed with an ABI Prism 7500 sequence detection system (Applied Biosystems) with Power SYBR Green PCR master mix (Applied Biosystems). Primer sequences are listed in *SI Appendix*, Table S1. Gene expression was usually normalized to *ACTB* gene, and in some cases to *CD8A*.

Flow Cytometry. Single-cell suspensions from tumors, Matrigel plugs, and peripheral blood were stained, using a Live/Dead Fixable Aqua Dead Cell Stain Kit (Invitrogen), for dead cell exclusion according to the manufacturer's instructions. Cells were submitted to the standard FACS staining procedures. For intracellular cytokine staining, a Cytofix/Cytoperm Fixation/Permeabilization Kit (BD Biosciences) was used. Abs against cell surface intracellular markers/cytokines are listed in *SI Appendix*, Table S2. FACS data were acquired using a BD FACSCanto II (BD Biosciences), and the data were analyzed using FlowJo (TreeStar, Inc.).

Measurement of CCL2. CCL2 concentration was measured in supernatants of 12-d 4T1 tumors after enzymatic digestion using a specific ELISA kit (Peprotech). The cytokine concentration was standardized to the total protein concentration, measured using a Protein Assay kit (Bio-Rad).

Immunohistochemistry (Frozen Sections). Samples from tumors were fixed in 4% paraformaldehyde for 6 h and equilibrated in a 20% sucrose solution for 24 h; they were then embedded in frozen tissue matrix (Tissue-Tek OCT). Sections (12-μm thick) were stained according to a standard protocol with anti-CD8 Abs (53-6.7; Biolegend) overnight. Secondary Abs conjugated with Cy-2 (Jackson ImmunoResearch) were used subsequently. Nuclei were counterstained with DAPI. Sections were examined under a Zeiss laser scanning confocal microscope.

TCGA Dataset. Linear regression analysis in breast cancer was performed in Prism (GraphPad) using the TCGA dataset (https://cancergenome.nih.gov/).

Statistical Analysis. Statistical analyses were performed using Prism. Significance of the results was determined using the unpaired *t* test. Each experiment was performed three to five times. Linear regression analysis in breast cancer was performed in Prism using the TCGA dataset.

ACKNOWLEDGMENTS. We thank Dr. Tali Feferman, The Wiezmann Institute, Rehovot, for initial supply of anti-PD-1; and Dr. Marina Bersudsky and Malka R. White, Ben-Gurion University, Beer-Sheva, for the technical support. This project was supported by Israel Cancer Association Grant 20110083 (to R.N.A. and E.V.), Israel Cancer Research Foundation Grant 17-1979-PG (to R.N.A., and E.V.), and Binational (Israel-USA) Science Foundation Grant 2011263 (to R.N.A., E.V., and M.R.S.). C.A.D. was supported by NIH Grant AI-15614. R.N.A. is an incumbent of the Irving Isaac Sklar Chair in Endocrinology and Cancer.

1. Voronov E, et al. (2013) Unique versus redundant functions of IL-1α and IL-1β in the tumor microenvironment. *Front Immunol* 4:177.
2. Voronov E, Apte RN (2017) Targeting the tumor microenvironment by intervention in interleukin-1 biology. *Curr Pharm Des* 23:4893–4905.
3. Hanahan D, Weinberg RA (2011) Hallmarks of cancer: The next generation. *Cell* 144: 646–674.
4. Maman S, Witz IP (2018) A history of exploring cancer in context. *Nat Rev Cancer* 18: 359–376.
5. Becht E, et al. (2016) Immune contexture, immunoscore, and malignant cell molecular subgroups for prognostic and theranostic classifications of cancers. *Adv Immunol* 130: 95–190.
6. Fridman WH, Zitvogel L, Sautès-Fridman C, Kroemer G (2017) The immune contexture in cancer prognosis and treatment. *Nat Rev Clin Oncol* 14:717–734.
7. Mlecnik B, et al. (2016) The tumor microenvironment and immunoscore are critical determinants of dissemination to distant metastasis. *Sci Transl Med* 8:327ra26.
8. Anani W, Shurin MR (2017) Targeting myeloid-derived suppressor cells in cancer. *Adv Exp Med Biol* 1036:105–128.
9. Beyer M, Schultze JL (2006) Regulatory T cells in cancer. *Blood* 108:804–811.
10. Fleming V, et al. (2018) Targeting myeloid-derived suppressor cells to bypass tumor-induced immunosuppression. *Front Immunol* 9:398.
11. Galdiero MR, Garlanda C, Jaillon S, Marone G, Mantovani A (2013) Tumor associated macrophages and neutrophils in tumor progression. *J Cell Physiol* 228:1404–1412.
12. Kitamura T, Qian BZ, Pollard JW (2015) Immune cell promotion of metastasis. *Nat Rev Immunol* 15:73–86.
13. Kumar V, Patel S, Tcyganov E, Gabrilovich DI (2016) The nature of myeloid-derived suppressor cells in the tumor microenvironment. *Trends Immunol* 37:208–220.
14. Ma Y, Shurin GV, Gutkin DW, Shurin MR (2012) Tumor associated regulatory dendritic cells. *Semin Cancer Biol* 22:298–306.
15. Mantovani A, Locati M (2013) Tumor-associated macrophages as a paradigm of macrophage plasticity, diversity, and polarization: Lessons and open questions. *Arterioscler Thromb Vasc Biol* 33:1478–1483.
16. Mougiakakos D, Choudhury A, Lladser A, Kiessling R, Johansson CC (2010) Regulatory T cells in cancer. *Adv Cancer Res* 107:57–117.
17. Murray PJ (2018) Nonresolving macrophage-mediated inflammation in malignancy. *FEBS J* 285:641–653.
18. Solinas G, Germano G, Mantovani A, Allavena P (2009) Tumor-associated macrophages (TAM) as major players of the cancer-related inflammation. *J Leukoc Biol* 86: 1065–1073.
19. Tanaka A, Sakaguchi S (2017) Regulatory T cells in cancer immunotherapy. *Cell Res* 27: 109–118.
20. Dinarello CA (2018) Overview of the IL-1 family in innate inflammation and acquired immunity. *Immunol Rev* 281:8–27.
21. Garlanda C, Dinarello CA, Mantovani A (2013) The interleukin-1 family: Back to the future. *Immunity* 39:1003–1018.
22. Carmi Y, et al. (2013) The role of IL-1β in the early tumor cell-induced angiogenic response. *J Immunol* 190:3500–3509.
23. Krelin Y, et al. (2007) Interleukin-1beta-driven inflammation promotes the development and invasiveness of chemical carcinogen-induced tumors. *Cancer Res* 67: 1062–1071.
24. Song X, et al. (2005) CD11b+/Gr-1+ immature myeloid cells mediate suppression of T cells in mice bearing tumors of IL-1beta-secreting cells. *J Immunol* 175:8200–8208.

25. Escobar P, et al. (2015) IL-1β produced by aggressive breast cancer cells is one of the factors that dictate their interactions with mesenchymal stem cells through chemokine production. *Oncotarget* 6:29034–29047.
26. Kolb R, Liu GH, Janowski AM, Sutterwala FS, Zhang W (2014) Inflammasomes in cancer: A double-edged sword. *Protein Cell* 5:12–20.
27. Okamoto M, et al. (2010) Constitutively active inflammasome in human melanoma cells mediating autoinflammation via caspase-1 processing and secretion of interleukin-1beta. *J Biol Chem* 285:6477–6488.
28. Qin Y, et al. (2011) Constitutive aberrant endogenous interleukin-1 facilitates inflammation and growth in human melanoma. *Mol Cancer Res* 9:1537–1550.
29. Wu TC, et al. (2018) IL1 receptor antagonist controls transcriptional signature of inflammation in patients with metastatic breast cancer. *Cancer Res* 78:5243–5258.
30. Holen I, et al. (2016) IL-1 drives breast cancer growth and bone metastasis in vivo. *Oncotarget* 7:75571–75584.
31. Guo B, Fu S, Zhang J, Liu B, Li Z (2016) Targeting inflammasome/IL-1 pathways for cancer immunotherapy. *Sci Rep* 6:36107.
32. Bruchard M, et al. (2013) Chemotherapy-triggered cathepsin B release in myeloid-derived suppressor cells activates the Nlrp3 inflammasome and promotes tumor growth. *Nat Med* 19:57–64.
33. Voigt C, et al. (2017) Cancer cells induce interleukin-22 production from memory $CD4^+$ T cells via interleukin-1 to promote tumor growth. *Proc Natl Acad Sci USA* 114:12994–12999.
34. Ben-Sasson SZ, et al. (2013) IL-1 enhances expansion, effector function, tissue localization, and memory response of antigen-specific CD8 T cells. *J Exp Med* 210:491–502.
35. Buqué A, et al. (2016) Trial Watch-Small molecules targeting the immunological tumor microenvironment for cancer therapy. *OncoImmunology* 5:e1149674.
36. Medler TR, Cotechini T, Coussens LM (2015) Immune response to cancer therapy: Mounting an effective antitumor response and mechanisms of resistance. *Trends Cancer* 1:66–75.
37. Pitt JM, et al. (2016) Targeting the tumor microenvironment: Removing obstruction to anticancer immune responses and immunotherapy. *Ann Oncol* 27:1482–1492.
38. Ridker PM, et al.; CANTOS Trial Group (2017) Effect of interleukin-1β inhibition with canakinumab on incident lung cancer in patients with atherosclerosis: Exploratory results from a randomised, double-blind, placebo-controlled trial. *Lancet* 390:1833–1842.
39. Griffith JW, Sokol CL, Luster AD (2014) Chemokines and chemokine receptors: Positioning cells for host defense and immunity. *Annu Rev Immunol* 32:659–702.
40. Shi C, Pamer EG (2011) Monocyte recruitment during infection and inflammation. *Nat Rev Immunol* 11:762–774.
41. Chitu V, Stanley ER (2006) Colony-stimulating factor-1 in immunity and inflammation. *Curr Opin Immunol* 18:39–48.
42. Watowich SS, Liu YJ (2010) Mechanisms regulating dendritic cell specification and development. *Immunol Rev* 238:76–92.
43. Ridker PM, et al.; CANTOS Trial Group (2017) Antiinflammatory therapy with canakinumab for atherosclerotic disease. *N Engl J Med* 377:1119–1131.
44. Dinarello CA (2018) An interleukin-1 signature in breast cancer treated with interleukin-1 receptor blockade: Implications for treating cytokine release syndrome of checkpoint inhibitors. *Cancer Res* 78:5200–5202.
45. Isambert N, et al. (2018) Fluorouracil and bevacizumab plus anakinra for patients with metastatic colorectal cancer refractory to standard therapies (IRAFU): A single-arm phase 2 study. *Oncoimmunology* 7:e1474319.
46. Becerra CPA, Cavaness K, Hoof PD, Celinski S (2018) Gemcitabine, nab-paclitaxel, cisplatin, and anakinra (AGAP) treatment in patients with non-metastatic pancreatic ductal adenocarcinoma (PDAC). *J Clin Oncol* 36(Suppl):449.
47. Franklin RA, et al. (2014) The cellular and molecular origin of tumor-associated macrophages. *Science* 344:921–925.
48. Movahedi K, et al. (2010) Different tumor microenvironments contain functionally distinct subsets of macrophages derived from Ly6C(high) monocytes. *Cancer Res* 70:5728–5739.
49. Menezes S, et al. (2016) The heterogeneity of $Ly6C^{hi}$ monocytes controls their differentiation into $iNOS^+$ macrophages or monocyte-derived dendritic cells. *Immunity* 45:1205–1218.
50. Geissmann F, et al. (2010) Development of monocytes, macrophages, and dendritic cells. *Science* 327:656–661.
51. Soria G, Ben-Baruch A (2008) The inflammatory chemokines CCL2 and CCL5 in breast cancer. *Cancer Lett* 267:271–285.
52. Stanley ER, Chitu V (2014) CSF-1 receptor signaling in myeloid cells. *Cold Spring Harb Perspect Biol* 6:a021857.
53. Huang B, et al. (2007) CCL2/CCR2 pathway mediates recruitment of myeloid suppressor cells to cancers. *Cancer Lett* 252:86–92.
54. Kersten K, et al. (2017) Mammary tumor-derived CCL2 enhances pro-metastatic systemic inflammation through upregulation of IL1β in tumor-associated macrophages. *Oncoimmunology* 6:e1334744.
55. Mantovani A (2017) Wandering pathways in the regulation of innate immunity and inflammation. *J Autoimmun* 85:1–5.
56. Ruffell B, et al. (2014) Macrophage IL-10 blocks CD8+ T cell-dependent responses to chemotherapy by suppressing IL-12 expression in intratumoral dendritic cells. *Cancer Cell* 26:623–637.
57. Bertagnolli MM, Lin BY, Young D, Herrmann SH (1992) IL-12 augments antigen-dependent proliferation of activated T lymphocytes. *J Immunol* 149:3778–3783.
58. Smyth MJ, Ngiow SF, Ribas A, Teng MW (2016) Combination cancer immunotherapies tailored to the tumour microenvironment. *Nat Rev Clin Oncol* 13:143–158.
59. Harizi H, Juzan M, Moreau JF, Gualde N (2003) Prostaglandins inhibit 5-lipoxygenase-activating protein expression and leukotriene B4 production from dendritic cells via an IL-10-dependent mechanism. *J Immunol* 170:139–146.
60. Schrey MP, Patel KV (1995) Prostaglandin E2 production and metabolism in human breast cancer cells and breast fibroblasts. Regulation by inflammatory mediators. *Br J Cancer* 72:1412–1419.
61. Sharma P, Allison JP (2015) Immune checkpoint targeting in cancer therapy: Toward combination strategies with curative potential. *Cell* 161:205–214.
62. Topalian SL, et al. (2012) Safety, activity, and immune correlates of anti-PD-1 antibody in cancer. *N Engl J Med* 366:2443–2454.
63. Littman DR (2015) Releasing the brakes on cancer immunotherapy. *Cell* 162:1186–1190.
64. Pardoll DM (2012) Immunology beats cancer: A blueprint for successful translation. *Nat Immunol* 13:1129–1132.
65. Postow MA, Callahan MK, Wolchok JD (2015) Immune checkpoint blockade in cancer therapy. *J Clin Oncol* 33:1974–1982.
66. Barrett DM, Teachey DT, Grupp SA (2014) Toxicity management for patients receiving novel T-cell engaging therapies. *Curr Opin Pediatr* 26:43–49.
67. Xu XJ, Tang YM (2014) Cytokine release syndrome in cancer immunotherapy with chimeric antigen receptor engineered T cells. *Cancer Lett* 343:172–178.
68. Horai R, et al. (1998) Production of mice deficient in genes for interleukin (IL)-1alpha, IL-1beta, IL-1alpha/beta, and IL-1 receptor antagonist shows that IL-1beta is crucial in turpentine-induced fever development and glucocorticoid secretion. *J Exp Med* 187:1463–1475.
69. Giavridis T, et al. (2018) CAR T cell-induced cytokine release syndrome is mediated by macrophages and abated by IL-1 blockade. *Nat Med* 24:731–738.
70. Hickish T, et al. (2017) MABp1 as a novel antibody treatment for advanced colorectal cancer: A randomised, double-blind, placebo-controlled, phase 3 study. *Lancet Oncol* 18:192–201.